Bridge-bond formation in aluminum and its alloys under high pressure

Cong Li [1,*] Wenge Yang [1] and H. W. Sheng [2,†]

[1] *Center for High Pressure Science and Technology Advanced Research, Shanghai 201203, People's Republic of China*

[2] *Department of Physics and Astronomy, George Mason University, Fairfax, Virginia 22030, USA*

(Received 12 January 2021; revised 17 June 2021; accepted 18 February 2022; published 1 March 2022)

Despite being a simple metal in which the free-electron model prevails, aluminum is known to exhibit peculiar bonding characteristics. In this work, we report a hitherto unexplored bonding behavior of Al through extensive first-principles modeling. Starting from liquid Al, we report that upon increasing pressure, electrons tend to localize between two nearest Al neighbors, forming a partitionable electronic center resembling a pseudoparticle that lies between the two Al atoms. This finding is further generalized to binary alloys containing Al under high pressure, as exemplified by an Al-Li intermetallic compound. The emergence of this bridge bonding under pressure is found to profoundly affect the physical properties of the materials, evidenced by anomalous property crossovers systematically explored in the Al-Li alloy. The finding of the anomalous electronic bonding behavior of Al described in this work will lay groundwork for interpreting and predicting physical behavior under extreme conditions.

DOI: 10.1103/PhysRevMaterials.6.033601

I. INTRODUCTION

Light elements and their compounds generally present extraordinary chemical bonding features. Aluminum (Al) is considered to approach an "ideal" metal or free-electron gas where electrons move freely without being affected by the metal ions. However, despite extensive experimental and theoretic studies [1–6], the exact bonding nature of Al remains a mystery and a consensus has not been reached concerning the electronic structure of its chemical bonds. Several bonding types have been proposed in the literature, including bridge bonding between nearest neighbors [5,6], octahedrally centered bonding [1], tetrahedrally centered bonding [2], and mixtures thereof. Not until recently was Nakashima *et al.* [7] able to demonstrate that a tetrahedral bond network exists in Al that accounts for the directional nature of its mechanical properties. In this bonding picture [7], electron density in the tetrahedral interstitial sites of fcc Al is found to be in excess of the superposition of unbound atoms' free-electrons. Electron localization in the interstitial sites of Al is even more pronounced under high pressure, manifested by the formation of an electride phase at above terapascal (TPa) pressure [8], which can be described by a host-guest model consisting of positive ions and interstitial electrons [9–11]. In fact, research on electrides has been a recurring theme in the literature. Similar to Al, many light metals such as Li [12–20], Na [21,22], and binary compounds [23–28] were found to form electrides under high pressure, which often possess unusual physical properties. The hallmark feature of the electrides is the formation of off-center lobes of electrons, also known as non-nuclear attractors (NNAs) [28,29], localized in the interstitial cavities.

In view of the bonding specification of Al, it is essential to explore its high-pressure bonding condition and see how it fares in its intermetallic compounds. In this paper, we report an unusual electron localization behavior of Al, where off-atom electrons are not localized in the interstitial sites, but instead lie directly between two Al atoms forming a type of electronic bonding.

Different from previous work, our strategy was to investigate bonding features in liquid Al under high pressure, which remains largely unexplored to date. On the one hand, knowledge of electronic bonding in liquid Al is essential to understanding its own structure and properties, and also furnishes crucial information for understanding other liquids at high pressure. On the other hand, the plural forms of local atomic packing environments in the liquid state provide otherwise unavailable opportunities to quantify the bonding characteristics. The bonding information about liquid Al we obtained was further scrutinized in its intermetallic alloys. To this end, considering that excess interstitial electrons exist in both elemental Al [8] and Li [7,12–20], and that additionally, the mixing of Al and Li can produce Li-Al compounds with Al in a high anionic charge state, we chose Li-Al as an ideal system for exploring the evolution of Al–Al bonding with an increasing amount of charges transferred to Al under high pressure. On a fundamental level, this work will provide insights into the structural evolution of Li-Al binary compounds under high-pressure conditions and uncover how the anomalous bonding affects the various physical properties, which remains unknown at this point.

II. COMPUTATIONAL METHODS AND DETAILS

Ab initio calculations were carried out in the density-functional theory-based Vienna *Ab initio* Simulation Package (VASP) code [30]. Liquid Al was studied with *ab initio* molecular dynamics in constant number, volume, and tem-

*cong.li@hpstar.ac.cn

†hsheng@gmu.edu

perature ensembles. To search for thermodynamically stable candidates of Li-Al compounds under pressure, we employed the swarm-intelligence based CALYPSO [31,32] structure prediction method. Superconducting properties were calculated based on the plane-wave pseudopotential method, as implemented in the QUANTUM ESPRESSO code [33]. Electrical conductivity was calculated using the BOLTZTRAP code [34] under constant relaxation time approximation. Detailed descriptions of the computational approaches can be found in Supplemental Material [35].

III. RESULTS AND DISCUSSIONS

At room temperature, Al with an fcc structure has been reported to be stable up to 200 GPa [36]. Here, to explore the bonding pattern of Al under high pressure, we conducted a series of calculations on the Bader charge [37] and electron localization function (ELF) [38] analysis of fcc Al under 100 GPa as shown in Fig. S1. The results clearly indicate that excess electron charges (the "bond") exist in the tetrahedral "holes," which agrees with the experimental findings of Nakashima *et al.* [7] at ambient condition.

Liquid Al, however, behaves drastically different under high pressure. At ambient pressure, it is generally regarded as a simple liquid within the hard-sphere paradigm, which can be described by a polytetrahedral assembly [39,40]. Each atom in the liquid is tightly coordinated by its 13 or 14 nearest neighbors, forming a coordination polyhedron consisting of a group of tetrahedra. Following the electronic-bonding picture for fcc Al, intuitively, one would expect the electrons to be localized in the centers of the tetrahedra at elevated pressures.

Our analysis revealed a different bonding pattern in liquid Al. Figure 1 summarizes our calculated results of liquid Al under 108 GPa and 4000 K. The electronic charge-density distributions [Figs. 1(a) and (1b)] reveal that valence electrons assemble in the centers of two nearest Al atoms, rather than the centers of the tetrahedra. By means of Bader charge analysis, we found that the excess electrons could be partitioned into (based on the zero-flux surface of the charge density) a volume separating them from the atoms. These off-atom electron lobes (or NNAs) are located approximately in the middle of two Al atoms, forming a pseudo-atomlike entity. To quantitatively demonstrate the location of the off-atom electron centers, we analyzed its radial distribution function with respect to Al. It can be seen in Fig. 1(c) that the distance from the NNA center (i.e., electron density maximum) to its nearest atomic position is roughly half of the nearest-neighbor Al distance. In this sense, the formation of an off-atom electron charge center has altered the original metallic bonding character of Al, seen as bridge bonding associated with Al-Al pairs. Put in a broader picture, evidently, the formation of these abundant off-atom electronic centers indicates that liquid Al belongs to a *liquid electride* at high pressure.

To further illustrate how this anomalous bonding is susceptible to pressure, we studied the bond formation probability as a function of Al-Al distance. As a measure of the incompressible core region, an ionic radius of 0.39 Å [41] was used for Al, whereas the size of the valence electron cloud is represented by the $3p$ orbital radius of 1.31 Å [42]. Our results revealed that for the given atomic packing environment, only

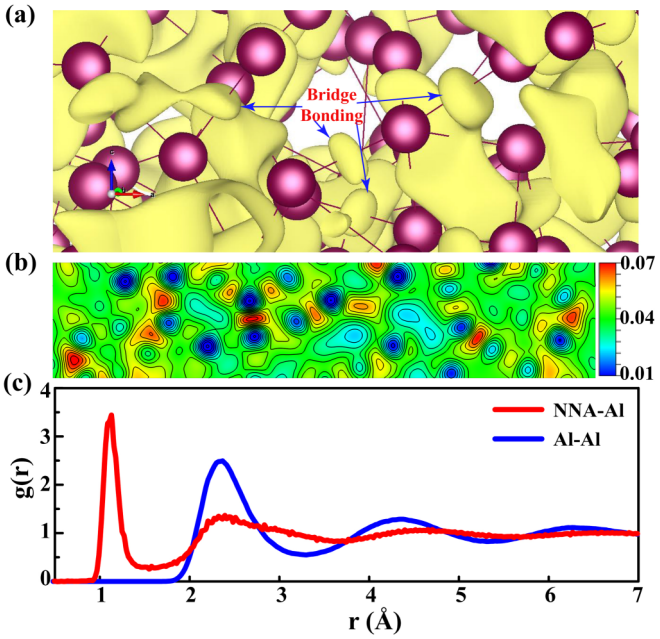

FIG. 1. Bonding properties of liquid Al at 108 GPa and 4000 K. (a) Electron charge-density isosurface ($0.052\,e/\text{Å}^3$) outlining the off-atom charges piled between two Al atoms (indicated by the blue arrows), forming anomalous bonding between Al-Al. (b) Charge-density map of a cut plane of liquid Al, showing charge-density maxima between two nearest Al atoms. The red zones correspond to the bridge charge. (c) Partial radial distribution functions of Al-Al and NNA-Al, showing the distance between NNA center and Al is half of the Al-Al nearest interatomic distance. NNA denotes the center of the off-atom charge lobes.

if the nearest Al-Al distance is shorter than the sum of the valence orbitals (2.62 Å) does the bridge bonding begin to appear, which is schematically illustrated in Fig. 2(a). We shall point out that the bridge-bonding centers appear in hot liquid Al even at relatively low pressures (see, e.g., Fig. S2 for liquid-Al at 13 GPa, 3000 K) because of reduced Al-Al pair distances at increased temperatures. Such a bonding behavior may be perturbed by electron charge-density fluctuations imposed by the disordered atomic arrangements in the liquid.

Now, we generalize this peculiar bonding feature of Al in a broad picture by tapping into the bonding characteristics of various Al-rich intermetallic compounds, i.e., materials containing Al but exhibiting multifarious atomic environments, using LiAl as an example. We show that a similar bonding pattern exists in Li-Al compounds under high pressures. To establish a high-pressure phase diagram of the Li-Al system and locate thermodynamically stable Li-Al phases, we performed an extensive search for the stable crystal structures of Li_xAl ($x = 1$, 1.5, 2, 2.5, 3, 3.5, and 4–8) within a pressure range of 0–100 GPa with a maximum simulation cell up to 4 formula units for each fixed composition. According to the formation enthalpy and the convex-hull approach, apart from the well-known compounds LiAl, Li_3Al_2, and Li_2Al, two stable compounds (Li_4Al and Li_6Al) were identified under high pressure [see Supplemental Material Fig. S3(a) and Table SI]. The pressure-composition phase diagram of the Li-Al system is shown in Fig. S3(b). All the atomic structures

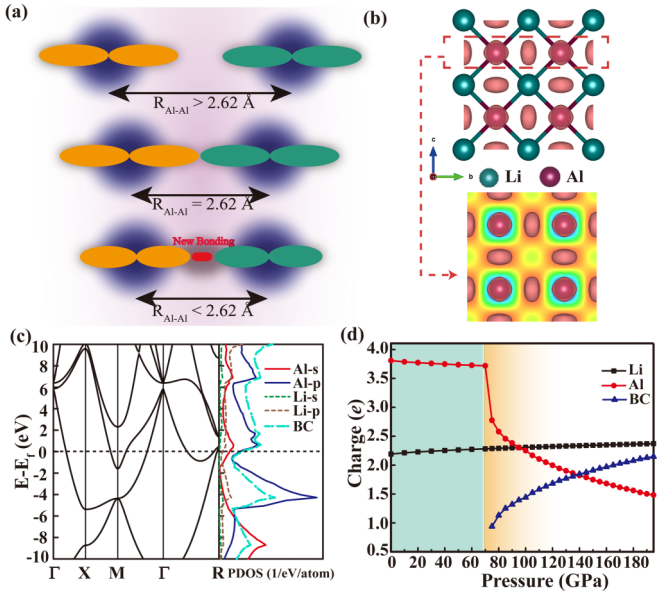

FIG. 2. (a) A schematic diagram showing the emergence of bonding between Al-Al atoms when the interatomic distance becomes shorter than a threshold. (b) Calculated ELF of *Pm*-3*m* LiAl with an isosurface value of 0.75 at 100 GPa, indicating an off-atom electron lobe bridge bonds two Al atoms (red spheres). (c) Electronic band structure and PDOS of *Pm*-3*m* LiAl at 100 GPa. The bridge charges have a *p*-electron character. (d) Bader charges of each entity in the *Pm*-3*m* LiAl crystal as a function of pressure. "BC" denotes the bridge charge associated with the NNA. Bridge bonding emerges at round 75 GPa.

of the stable phases under high pressure were proven to be dynamically stable, as they did not show imaginary frequency modes (Fig. S4).

We turn our focus to the equiatomic Li-Al compounds. The stable *Fd*-3*m* LiAl compound morphed into a cubic phase with the *Pm*-3*m* symmetry above 22 GPa, which was predicted to be stable up to 200 GPa in this work. The electronic structure of the most stable *Pm*-3*m* LiAl phase at high pressures was analyzed by Bader charge analysis and ELF. The calculated ELF [Fig. 2(b)] of *Pm*-3*m* LiAl under 100 GPa characterizes that the localization of excess electrons is in the center of two nearest Al atoms. The electronic bands and projected densities of states (DOS) of *Pm*-3*m* LiAl in Fig. 2(c) show that this phase still exhibits a metallic feature under 100 GPa. Moreover, the conducting states of *Pm*-3*m* LiAl derive mainly from the Al-3*p* states around the Fermi level. We also analyzed the DOS of the NNAs involved in the bridge bonding. The NNA can be seen as a pseudoparticle in the lattice of the *Pm*-3*m* structure under 100 GPa. The obtained PDOS curves are shown in Fig 2(c). We note that the contribution of the NNAs to the electron DOS is larger than that of the Al and Li atoms near the Fermi surface. To further understand the origin of the bridge bonding, the charge transfer of *Pm*-3*m* structure under different pressures was analyzed by the Bader analysis depicted in Fig. 2(d). At low pressures ($P < 70$ GPa), the Bader charges of Li and Al are almost constant within the pressure range, about 2.25 *e* and 3.75 *e*, respectively. Upon the formation of bridge bonds, the Bader charge of Al decreases sharply, as opposed to that of Li,

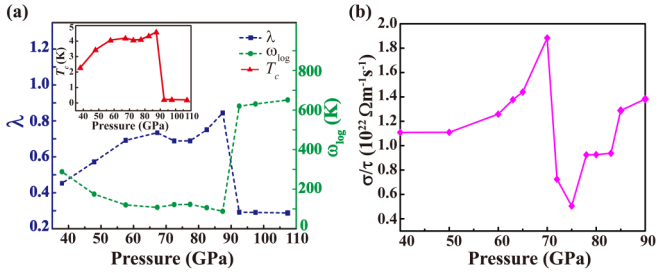

FIG. 3. The superconductive and conductive properties of *Pm*-3*m* LiAl as a function of pressure. (a) The electron-phonon coupling coefficient and the logarithmic average phonon frequency ω_{log} as a function of pressure. The inset shows the superconducting critical temperature T_c as a function of pressure. (b) Electrical conductivity σ/τ as a function of pressure at 300 K. Upon the formation of bridge bonding, the electrical conductivity shows a sudden drop.

which essentially remains steady when the pressure is above 70 GPa. Around this inflection pressure point, however, abrupt changes of both the band structure and the Fermi surface were not observed (Fig. S5).

Our calculations thus reveal that excess electrons pile into the center of two nearest Al atoms under pressure, promoting the formation of bridge bonding. These bridge-bonding charges are provided mainly by Al atoms, evidenced by the fact that the integrated charges of Li atoms remain basically unchanged. More specifically, at low pressures, there is a small amount of charge transferred from Li to Al (∼0.75 *e* per Li atom). Upon increasing the pressure to above 70 GPa, the 3*p* electrons of Al atoms start to be trapped between two nearest Al neighbors, forming an NNA. In other words, Al atoms gradually reach an ionic state, and nearly two electrons reside in the centers of the Al-Al pairs to form bridge bonds in the unit cell. To demonstrate this, a hypothetical $[LiAl]^{2+}$ model system was investigated by explicitly removing two electrons from the *Pm*-3*m* LiAl crystal. The absence of Bader charge in the center of the Al-Al atoms (Table SII) confirms that those electrons of Al atoms are responsible for the formation of bridge bonds. Other Al-based intermetallic compounds (Supplemental Material, Fig. S6) have also been investigated and were found to exhibit similar bridge-bonding features under certain pressure conditions. To further validate the generality of Al-Al bridge bonding, we studied the electronic bonding feature of *liquid* $Al_{50}Li_{50}$ at high pressures as well, and the results are provided in Fig. S7. Analogous to liquid Al, in the liquid $Al_{50}Li_{50}$, electrons were found to convene between Al-Al pairs in lieu of the tetrahedral interstitials as depicted in other high-pressure electrides.

The high-pressure bonding behavior of Al described above is characteristically different from previously known ionic, covalent, and metallic bonding types. We heuristically explored how the physical properties are affected by the discovered bridge bonding. In what follows, we will examine the electron transport, mechanical, and thermal properties of the Li-Al compounds and demonstrate that the properties are substantially impacted by the formation of bridge bonds.

We first illustrate the superconducting transition temperature (T_c) through electron-phonon coupling (EPC). Here, we take *Pm*-3*m* LiAl as an example. As shown in Fig. 3(a), the

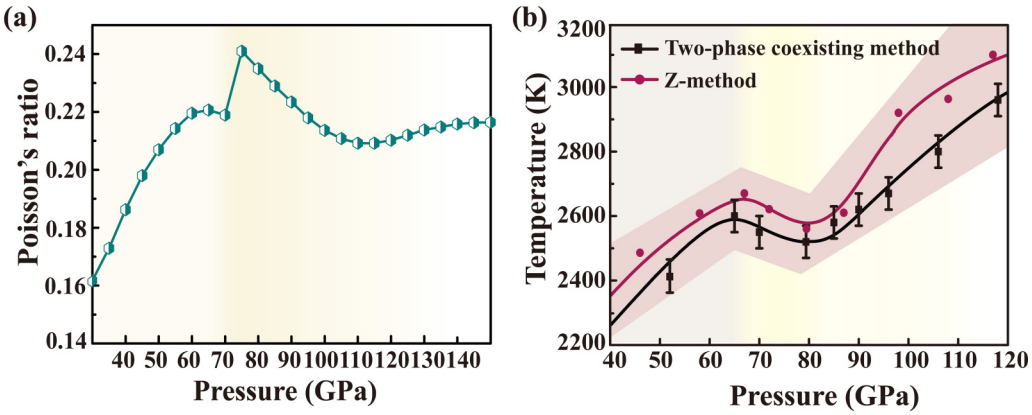

FIG. 4. The mechanical properties and melting points of *Pm*-3*m* LiAl as a function of pressure. (a) Poisson's ratio and (b) melting points. Error bars correspond to the calculated melting-point uncertainty of ±50 K [35] by two-phase coexisting method. Property crossovers are identified as a result of the formation of bridge bonds.

EPC constant λ and the logarithmic average phonon frequency $\omega_{\log}$ change sharply between 75–90 GPa. Consequently, T_c decreases sharply from 4.58 to 0.23 K at around 90 GPa. A sharp drop indicates that the state of intrinsic charge concentration has changed at the corresponding pressure, which is near the bridge-bond formation pressure at 75 GPa. Concurrently, similar results were found for the electrical conductivity as shown in Fig. 3(b), where the electrical conductivity σ/τ increases first with external pressure and then sudden decreases above 75 GPa. Hence, the formation of the bridge bonding has a paramount importance for the superconducting transition temperature T_c and conductivity. Likewise, the thermal conductivity of LiAl was also found to be affected by the formation of bridge bonds (results not shown).

The mechanical properties of these phases under high pressure were studied by computing the elastic constants and moduli using linear response theory [43]. The elastic constants of Pm-3*m* LiAl change dramatically at 75 GPa, leading to a jump of the shear modulus. This change is more obvious in the Poisson ratio [Fig. 4(a)] in this pressure range. To assess the thermal properties, we calculated the melting temperatures of *Pm*-3*m* LiAl by two complementary *ab initio* approaches (see Supplemental Material for details) as shown in Fig. 4(b) and found a reentrant behavior in a similar pressure range in which the mechanical properties show anomalies. The melting points calculated with the two different methods show a consistent trend. Unlike the normal melting curve of elements (e.g., transition metals), the melting points of LiAl with increasing pressure show a zigzag shape, which increases monotonically up to 68 GPa, followed by a decrease from 68 to 80 GPa, and then a normal increase again at higher pressures. It is noticeable that the pressure range of the anomalous change of melting points is between 68 and 80 GPa, which coincides with the pressures for the formation of bridge bonds. Therefore, the consistency in the changes of the electronic properties, mechanical properties, and melting curve proves that the bridge bonding has unexpected effects on the physical properties of materials.

IV. CONCLUSION

In summary, we performed a systematic search for the bonding pattern of liquid Al and its intermetallic alloys under high pressure, among which Li-Al compounds were illustrated as an archetypal example. We found that electrons assemble into the center of two Al nearest neighbors to form a bridge-type bonding under high pressure in liquid Al and its compounds. The formation of bridge bonding was attributed to the overlap of the *3p* orbitals of two nearest-neighbor Al atoms that causes the *p* electrons of Al to be localized in the center of the two atoms. The physical properties were found to be profoundly affected by the formation of bridge bonds, as exemplified by their superconducting transition temperature, mechanical properties, and melting points. Phenomenologically, the continuous electronic transition associated with the bridge-bond formation loosely resembles the spin crossover reported in ferropericlase under high pressure [44,45] that also occurs in a broad temperature and pressure range and leads to substantial properties changes. Our current findings will shed light on the bonding behavior of light elements in general, and also help understand electronic structure and material properties under high pressure.

ACKNOWLEDGMENTS

The calculations in this work were performed at the Tianhe II supercomputer in Guangzhou and on Hefei advanced computing center. C.L. is highly grateful for insightful discussions with Dr. Chris J. Pickard and Dr. Xiao Dong. This work was partially supported by the National Nature Science Foundation of China under Grants No. U1930401.

[1] S. Ogata, J. Li, and S. Yip, Science **298**, 807 (2002).
[2] N. Kioussis, M. Herbranson, E. Collins, and M. E. Eberhart, Phys. Rev. Lett. **88**, 125501 (2002).
[3] A. G. Fox, M. A. Tabbernor, and R. M. Fisher, J. Phys. Chem. Solids **51**, 1323 (1990).
[4] N. Sirota, Acta Crystallogr. A **25**, 223 (1969).

[5] S. Chakraborty, A. Manna, and A. K. Ghosh, Phys. Status Solidi B **129**, 211 (1985).
[6] E. Rantavuori and V. P. Tanninen, Phys. Scr. **15**, 273 (1977).
[7] P. N. H. Nakashima, A. E. Smith, J. Etheridge, and B. C. Muddle, Science **331**, 1583 (2011).
[8] C. J. Pickard and R. J. Needs, Nat. Mater. **9**, 624 (2010).
[9] J. L. Dye, Acc. Chem. Res. **42**, 1564 (2009).
[10] J. L. Dye, Science **247**, 663 (1990).
[11] B. Rousseau and N. W. Ashcroft, Phys. Rev. Lett. **101**, 046407 (2008).
[12] J. Lv, Y. Wang, L. Zhu, and Y. Ma, Phys. Rev. Lett. **106**, 015503 (2011).
[13] M. Marques, M. I. McMahon, E. Gregoryanz, M. Hanfland, C. L. Guillaume, C. J. Pickard, G. J. Ackland, and R. J. Nelmes, Phys. Rev. Lett. **106**, 095502 (2011).
[14] J. B. Neaton and N. W. Ashcroft, Nature (London) **400**, 141 (1999).
[15] M. Hanfland, K. Syassen, N. E. Christensen, and D. L. Novikov, Nature (London) **408**, 174 (2000).
[16] Y. Yao, J. S. Tse, and D. D. Klug, Phys. Rev. Lett. **102**, 115503 (2009).
[17] G. Profeta, C. Franchini, N. N. Lathiotakis, A. Floris, A. Sanna, M. A. L. Marques, M. Lüders, S. Massidda, E. K. U. Gross, and A. Continenza, Phys. Rev. Lett. **96**, 047003 (2006).
[18] T. Matsuoka and K. Shimizu, Nature (London) **458**, 186 (2009).
[19] C. J. Pickard and R. J. Needs, Phys. Rev. Lett. **102**, 146401 (2009).
[20] C. L. Guillaume, E. Gregoryanz, O. Degtyareva, M. I. McMahon, M. Hanfland, S. Evans, M. Guthrie, S. V. Sinogeikin, and H. K. Mao, Nat. Phys. **7**, 211 (2011).
[21] Y. Ma, M. Eremets, A. R. Oganov, Y. Xie, I. Trojan, S. Medvedev, A. O. Lyakhov, M. Valle, and V. Prakapenka, Nature (London) **458**, 182 (2009).
[22] J. S. Tse, Natl. Sci. Rev. **7**, 149 (2020).
[23] Z. Zhao, S. Zhang, T. Yu, H. Xu, A. Bergara, and G. Yang, Phys. Rev. Lett. **122**, 097002 (2019).
[24] S. Shao, W. Zhu, J. Lv, Y. Wang, Y. Chen, and Y. Ma, npj Comput. Mater. **6**, 11 (2020).
[25] X. Zhong, M. Xu, L. Yang, X. Qu, L. Yang, M. Zhang, H. Liu, and Y. Ma, npj Comput. Mater. **4**, 70 (2018).
[26] H. Tang, B. Wan, B. Gao, Y. Muraba, Q. Qin, B. Yan, P. Chen, Q. Hu, D. Zhang, L. Wu, M. Wang, H. Xiao, H. Gou, F. Gao, H. Mao, and H. Hosono, Adv. Sci. **5**, 1800666 (2018).
[27] B. Wan, S. Xu, X. Yuan, H. Tang, D. Huang, W. Zhou, L. Wu, J. Zhang, and H. Gou, J. Mater. Chem. A **7**, 16472 (2019).
[28] X. Dong, A. R. Oganov, A. F. Goncharov, E. Stavrou, S. Lobanov, G. Saleh, G. Qian, Q. Zhu, C. Gatti, V. L. Deringer, R. Dronskowski, X. Zhou, V. B. Prakapenka, Z. Konôpková, I. A. Popov, A. I. Boldyrev, and H. Wang, Nat. Chem. **9**, 440 (2017).
[29] J. Cioslowski, J. Phys. Chem. **94**, 5496 (1990).
[30] G. Kresse and J. Furthmüller, Phys. Rev. B **54**, 11169 (1996).
[31] Y. Wang, J. Lv, L. Zhu, and Y. Ma, Phys. Rev. B **82**, 094116 (2010).
[32] Y. Wang, J. Lv, L. Zhu, and Y. Ma, Comput. Phys. Commun. **183**, 2063 (2012).
[33] P. Giannozzi, S. Baroni, N. Bonini, M. Calandra, R. Car, C. Cavazzoni, D. Ceresoli, G. L. Chiarotti, M. Cococcioni, and I. Dabo, J. Phys.: Condens. Matter **21**, 395502 (2009).
[34] G. K. H. Madsen and D. J. Singh, Comput. Phys. Commun. **175**, 67 (2006).
[35] See Supplemental Material at http://link.aps.org/supplemental/10.1103/PhysRevMaterials.6.033601 for computational details; Fig. S1-7; and Table SI-II.
[36] D. N. Polsin, D. E. Fratanduono, J. R. Rygg, A. Lazicki, R. F. Smith, J. H. Eggert, M. C. Gregor, B. H. Henderson, J. A. Delettrez, R. G. Kraus, P. M. Celliers, F. Coppari, D. C. Swift, C. A. McCoy, C. T. Seagle, J.-P. Davis, S. J. Burns, G. W. Collins, and T. R. Boehly, Phys. Rev. Lett. **119**, 175702 (2017).
[37] E. Sanville, S. D. Kenny, R. Smith, and G. Henkelman, J. Comput. Chem. **28**, 899 (2007).
[38] A. D. Becke and K. E. Edgecombe, J. Chem. Phys. **92**, 5397 (1990).
[39] D. R. Nelson and F. Spaepen, Solid State Phys. **42**, 1 (1989).
[40] A. V. Anikeenko and N. N. Medvedev, Phys. Rev. Lett. **98**, 235504 (2007).
[41] R. D. Shannon and C. T. Prewitt, Acta Crystallogr. **25**, 925 (1969).
[42] J. T. Waber and D. T. Cromer, J. Chem. Phys. **42**, 4116 (1965).
[43] S. Baroni, P. Giannozzi, and A. Testa, Phys. Rev. Lett. **59**, 2662 (1987).
[44] E. Holmström and L. Stixrude, Phys. Rev. Lett. **114**, 117202 (2015).
[45] Z. Wu and M. W. Renata, Proc. Natl. Acad. Sci. USA. **111**, 10468 (2014).